

FUNDAMENTALS OF MECHANICAL ALLOYING

J.S. Benjamin

Aluminum Company of America, Alcoa Laboratories
Alcoa Center, PA, USA

ABSTRACT

The mechanical alloying process was developed some 25 years ago for the production of oxide dispersion strengthened superalloys. Early understanding of the process was empirical and limited by analytical techniques available at the time. The present paper reviews the phenomenology of the process based on knowledge gathered from the earliest experiments to the present. As originally practiced, the process utilized high energy ball mills for the processing of mixtures of elemental and master alloy powders to which fine oxide powders had been added. Since then, the process has been used cryogenically, with grinding aids, to process prealloyed powders, and, more recently with devices other than impact mills. These variations of the process will be discussed and an attempt made to elucidate opportunities for further enhancements in the understanding of the process and for widening of its utility.

INTRODUCTION

The original mechanical alloying process was the by-product of research into a different subject. Work at the International Nickel Company's Paul D. Merica Research Laboratory in the early 1960s had demonstrated that an aluminum-based analog of cast iron could be produced by injecting nickel coated graphite particles into molten aluminum alloys using an argon sparging gas. Attempts were made to inject nickel coated refractory oxide particles into nickel based superalloys in an effort to

produce an alloy combining the benefits of oxide dispersion strengthening with gamma prime precipitation hardening for high temperature applications. A number of different processes were studied for production of the coated fine oxides required for this injection process. These processes included co-reduction of mixed oxides of nickel and thorium and ball milling of various oxides with nickel in order to form a coating of the ductile metal on the oxide much as is done in the production of tungsten carbide-cobalt composite materials. The ball milling process in particular was used to coat oxides with metals that could not be applied by chemical processes due to their reactivity. For example, zirconium oxide was coated with aluminum in one such experiment. Since the apparatus employed, a small high energy vibratory mill, could produce only 1 cm³ of powder per run, these powders were used only for studies of the rate of rejection of oxide powders from molten alloys. Compacts of the composite powders were partially melted in an arc melter, sectioned and examined metallographically.

Because the rejection of unwetted oxide particles from molten nickel based superalloys was extremely rapid, this project was ultimately unsuccessful. However, a number of key ideas developed in this effort "congealed" to offer an alternative way to achieve the original goal. These concepts included the fact that both welding and fracturing occur during the ball milling of metallic powders. Second, high energy mills such as vibratory mills and stirred ball mills can greatly increase the rate of the grinding and fracturing processes. Third, virtually any composition could be manufactured using a mixture of elemental and readily available master alloy powders instead of having to rely on atomized prealloy powders, which were relatively rare and expensive at the time. Fourth, the thermodynamic activity of reactive gamma prime forming elements such as aluminum and titanium could be reduced orders of magnitude by combining them with noble metals such as nickel in intermetallic compounds. These intermetallic compounds were conveniently brittle and easily ground to fine powders. Fifth, by carrying out the processing in a dry condition, the welding part of the metal grinding operation could be enhanced at the expense of the fracturing component.

These key ideas led to the concept of establishing a "kneading" action which would refine the internal structure of powders while maintaining their overall particle size at a relatively coarse level preventing pyrophoricity.

BASIC ELEMENTS OF THE PROCESS

Mechanical alloying is a method for producing composite metal powders with a controlled fine microstructure. It occurs by the repeated fracturing and rewelding of a mixture of powder particles in a highly energetic ball charge. As originally carried out, the process requires at least one fairly ductile metal to act as a host or binder. Other components can consist of other ductile metals, brittle

metals and intermetallic compounds or nonmetals and refractory compounds. The process is usually carried out in high energy ball mills such as vibratory mills, stirred attritor-type ball mills or large conventional ball mills.

A mixture of powders and grinding media, with ratios ranging from 3:1 to 50:1 of balls to powder by volume, is employed. During agitation of this mixture, many powder particles are caught between the colliding grinding balls during each collision. Typically for the processing of nickel-based superalloys, a ball-to-powder ratio of 20:1 has been employed using hardened steel grinding balls with diameters of 0.75 cm. At an intermediate stage in the processing of such material, powder size distributions and geometrical considerations suggest that during each collision $\sim 1,000$ powder particles are involved, having a total mass of about 2×10^{-4} g. The greater number of such particles, about 75%, lie between the sizes of 10 and 30 μ . However, the bulk of the weight, 77%, lies between 30 and 100 μ .

Typical raw materials for the production of a simple nickel based superalloy are shown in figure 1. The large regular light colored particles are chromium. The intermediate sized gray particles are Ni-Al-Ti master alloy. The small spherical particles are carbonyl nickel. Submicron Y_2O_3 is also present but is not resolved at this magnification. As an aggregate mixture of these powder particles is trapped between the colliding grinding balls, it undergoes severe plastic deformation. This rup-



Figure 1 Raw materials for production of a nickel based superalloy: spherical carbonyl nickel (4-7 μ m), light chromium (50 to 150 μ m) and nickel-aluminum-titanium master alloy (20 to 100 μ m). Also present is submicrometer Y_2O_3 not visible at this magnification.

tures the adsorbed surface contaminant layers on each powder particle exposing fresh metal surface. Where powder particles overlap, metallurgical bonds are formed leading to particle growth and the formation of composite particles. Such composite particles are shown in figure 2 after 1.5 hrs of processing. The original ingredients are readily identified within each composite particle. As processing continues (figure 3), the internal structure of the powders continues to be refined. The average particle size of the powders, however, is actually increased from the initial average particle size of less than $20\ \mu$ to something in the order of $80\ \mu$. See figure 4. The initial particle size was dominated by the relatively large fraction of $4\text{-}7\ \mu$ nickel powders. In addition, the microhardness of the powders is increased from a starting value of $\sim 450\ \text{kg/mm}^2$ to $\sim 550\ \text{kg/mm}^2$ at this stage of processing. See figure 5. With extended processing, in this case 40 hrs, the internal structure of the powder particles is sufficiently refined that few features can be discerned by optical metallography. See figure 6. The hardness has reached saturation value of $\sim 750\ \text{kg/mm}^2$ while the average particle size has reached a steady state value of between 100 and $130\ \mu$.

To account for the establishment and maintenance of a steady state particle size distribution in the face of obvious continued severe plastic deformation demonstrated by the refinement of internal structure, one must explain why finer particles are preferentially welded and coarser particles tend to be fragmented into smaller particles. It stands to reason that while fracturing can be propagated incrementally by a series of successive impact events, the welding must occur with a single event to prevent reocclusion of fresh metal surface by exposure to the milling atmosphere. This can be

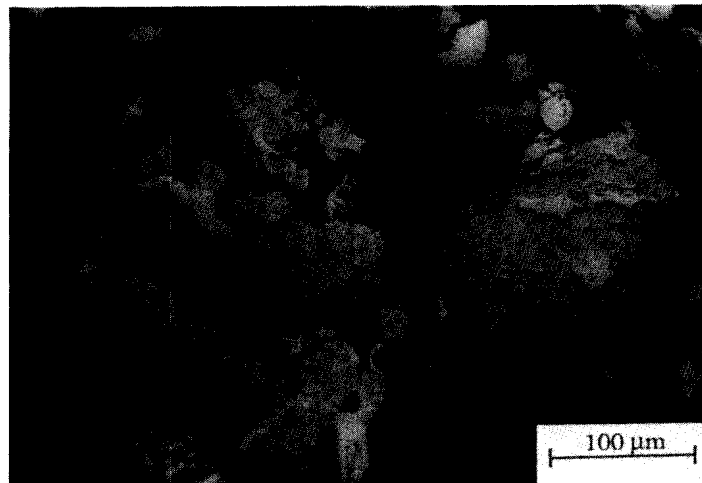


Figure 2 Superalloy powder early in the process, 1.5 hrs.

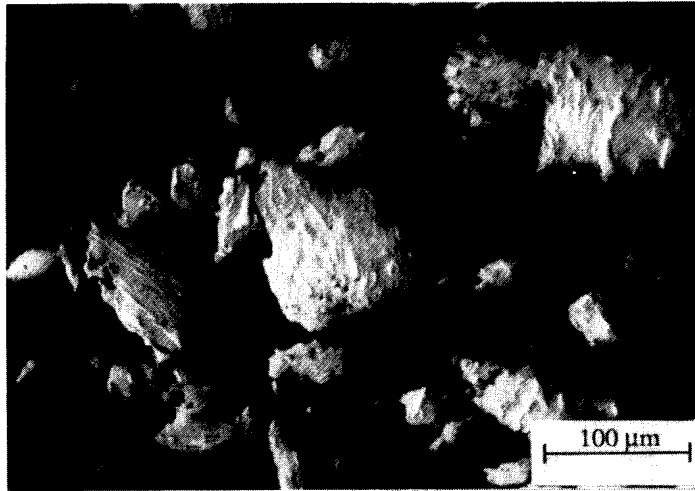


Figure 3 Superalloy powder after 3.5 hrs of processing.

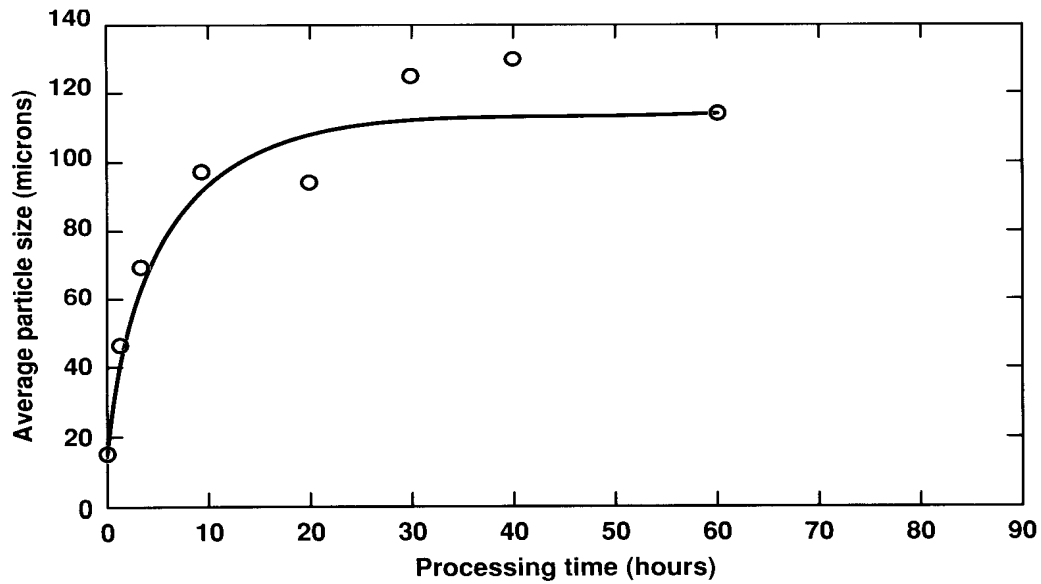


Figure 4 Particle size of superalloy powders as a function of mechanical alloying processing time.

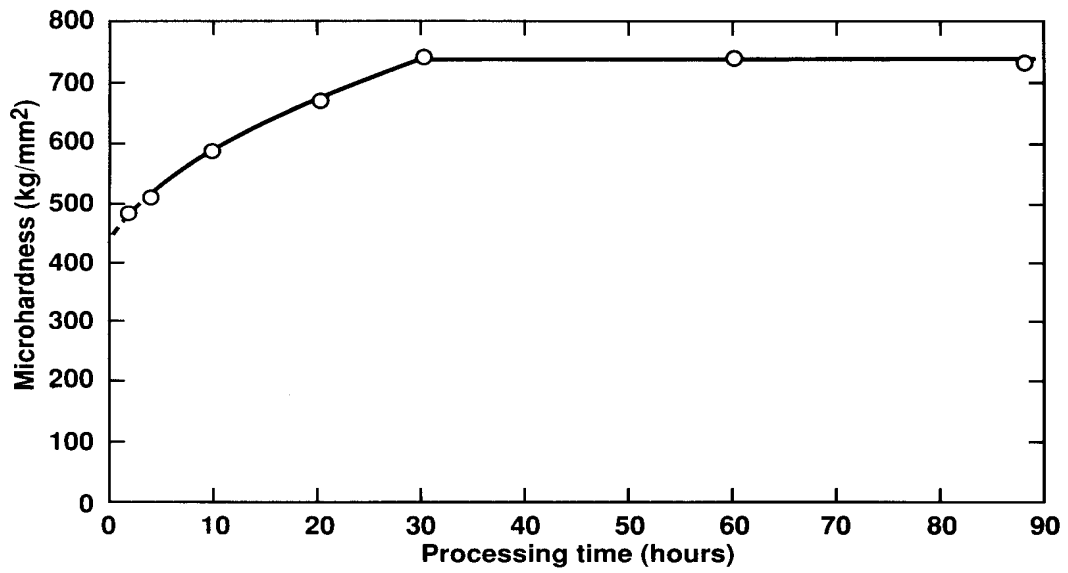


Figure 5 Microhardness of superalloy powders as a function of processing time.

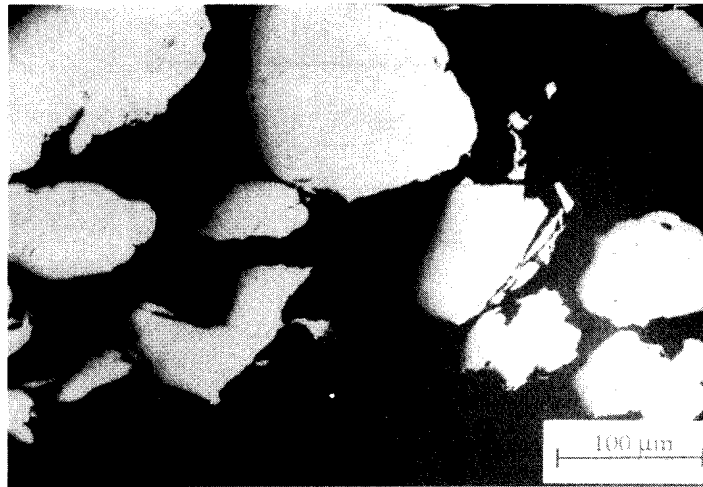


Figure 6 Mechanically alloyed superalloy powder at completion of 40 hrs of processing.

explained by assuming that each powder particle contains a distribution of flaws typical of brittle materials (see figure 7). Based on this hypothesis, large powder particles are more likely to contain at least one severe flaw while very small particles are less likely to contain a severe flaw and more likely to be able to withstand the severe strain required for welding. This is depicted schematically in figure 8 which shows the variation of ϵ_f , the fracture strain, as a function of particle size. The 2.5 and 97.5 percentile lines are also given indicating that this is a statistical variable. A horizontal line has been drawn at a value of ϵ_w representing the strain required for cold welding. Experiments on the mechanical alloying a mixture of iron and chromium and on pressure welding of macroscopic sheet suggests that this value is between 0.9 and 1.6. The particle size at which this line intersects the mean strain at fracture curve is significant. Particles smaller than this will tend to be welded while those coarser will tend to be fractured as indicated in the drawing. The reason for the initial increase in particle size in the example shown (figure 4) with increasing processing time can be explained by reference to the hardness curve. At early stages in the process the powders are quite ductile (as also evidenced by their plate-like shape). Only as they approach the saturation hardness value is the equilibrium distribution of flaws established.

While the increasing tendency for fracturing limits the maximum particle size in the distribution, there is another constraint. Simple energetic considerations indicate that the energy required to weld

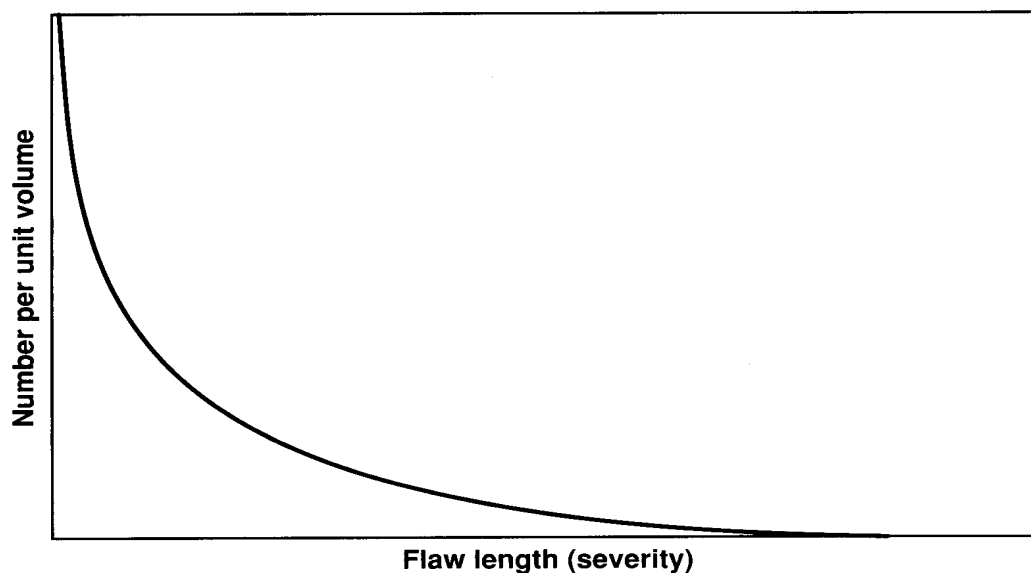


Figure 7 Schematic distribution of flaw severity in mechanically alloyed powder.

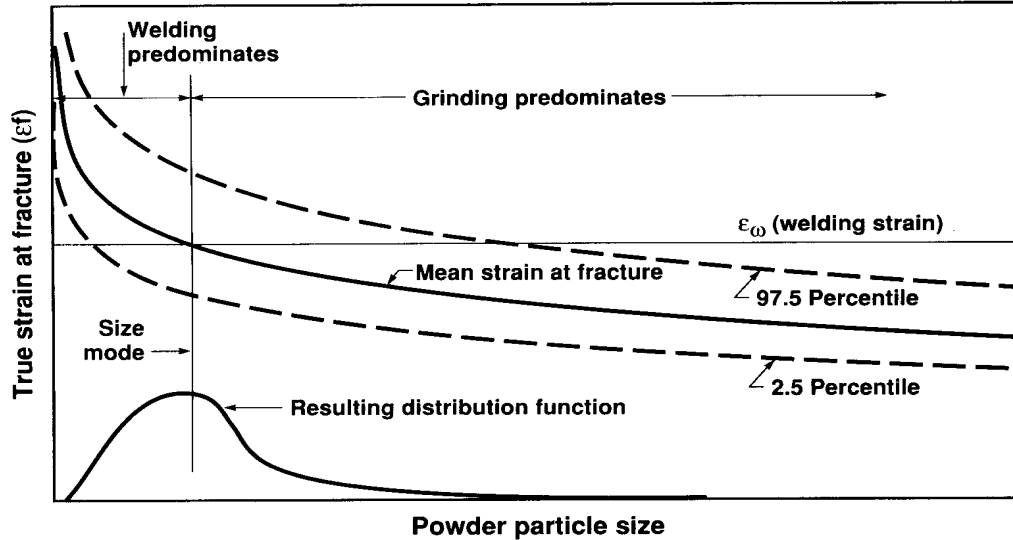


Figure 8 Schematic representation of particle size stabilization.

the particle, to cause a strain of from 0.9 to 1.6 in a single blow, is proportional to the volume of particle. When the volume of the largest particles exceed the maximum grinding ball energy, these particles will simply be hammered until they are reduced in size by the incremental propagation of internal flaws.

The fact that a saturation hardness is established (see figure 5) which stays constant with processing times of up to 90 hrs in the example shown suggests that some kind of work softening or diffusion process must be occurring in the powders, although the processing temperatures are relatively low, 100-200°C under most conditions. This has been confirmed for nickel-chromium alloys [1] and 70 copper-30 zinc brass [2] by both magnetic and X-ray measurements. This alloying can lead to the formation of solid solutions as in the two cases above or the formation of intermetallic compounds [3] or even amorphous materials [4]. The intermetallic compounds may first be formed as lamellae of their constituent elements are brought into closer contact and then destroyed by subsequent processing leading to amorphous phase formation. In fact, the developing refined composite powder particles consist of myriad microdiffusion couples.

The rate of refinement of structure has been tracked optically, by transmission electron microscopy and, at advanced stages, by X-ray line defraction. Figure 9 [1] shows the rate of refinement of struc-

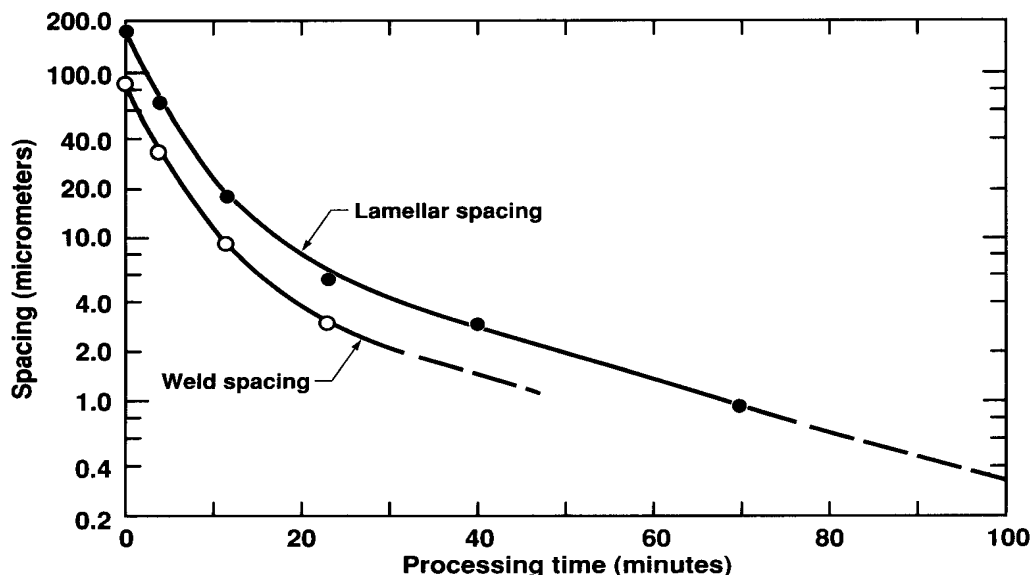


Figure 9 Lamellar thickness as a function of processing time in iron chromium powder processed in a shaker mill.

ture of a mixture of 50 vol.% iron-50 vol.% chromium processed in a high speed shaker mill. The initial powder particle size was between 74 and 105 μm . The weld spacing represents the distance between the surfaces of original chromium and original iron particles. The lamellar spacing is the distance between successive boundaries of iron to chromium and iron to chromium. This distance is therefore approximately twice the welding spacing. As might be expected for a process with a constant energy input rate and geometry of entrapment, refinement proceeds in a roughly logarithmic fashion. The initially high rate is due to the relatively low hardness of the powder at early stages in the processing and decreases with time. Once saturation hardness is achieved, after ~ 20 min in this case, the rate of change of the lamellar spacing became more nearly logarithmic with time. Transmission electron microscopy of processed particles of nickel based superalloys [5] showed linear features on the order of 0.1 μm or less after complete processing. X-ray diffraction analysis also confirmed the existence of minute fragments of slow diffusing alloying starting materials such as tungsten.

This continual refinement of original starting materials can no longer be followed as the spacing passes somewhere below 100 nanometers in thickness [6]. In appropriate systems, it is in this range that nanocrystalline or amorphous structures are formed. X-ray line broadening has been employed

to track structure below this. Materials processed to this degree exhibit increases in lattice parameter and a leveling off of the apparent crystallite size at around 10 nanometers. It is likely that, in complex systems such as nickel based superalloys which have many different ingredient compositions and particle sizes, portions of individual powder particles in the entire powder mass are at various stages of the development of structure at any given time. This is particularly so in the case of nickel based superalloys because as much as 60% of the volume of the powder is only 4-7 μm in size to begin with. It is also likely that, as has been shown for systems such as nickel-chromium and copper-zinc, both elements being relatively rapid diffusing, effective homogenization occurs at much shorter processing times than for systems such as copper-tantalum, in which one alloying element is a relatively slow diffuser. The reported increase in lattice parameter, the highly distorted microstructures with high dislocation densities, and the extremely high hardnesses of the powders are all consistent with enhanced diffusion capability which would also contribute to homogenization on an atomic scale long before the lamellar spacing had reached such a point. As structural features approach 10 nanometers, a balance is apparently achieved between the mechanical destruction of the structure and diffusive processes.

Attempts have been made recently [7,8] to model the mechanical alloying event. In these models, the authors calculate the collision time on the basis of the elastic encounter between steel grinding media and the temperature based on adiabatic heating of the plastically deformed powder elements during the collision event. The impact time was estimated as $\sim 10^{-5}$ sec. Cooling of the powder particle following the adiabatic heating was assumed to be based on transfer of heat from the particle to the surrounding milling atmosphere by Newtonian cooling. The authors estimated the heat transfer time at $\sim 10^{-2}$ sec.

In unpublished work by the present author, an alternative approach was taken. In this case it was assumed that the collision time was determined by the rate of deceleration of the grinding media by the plastically deforming metal particles trapped between them. Like the work in references 7 and 8, as an initial assumption, the collision was taken to be adiabatic. The example used was for a powder particle of cylindrical shape with both diameter and height equal to 100 μm and composed of a nickel based superalloy at saturation hardness. The variation of strength with temperature was modelled assuming that it was one-third the hardness at room temperature and gradually approached the strength of the consolidated alloy at 1200°C. On this basis, the powder strength was assumed to be 2,400 MPa at 20°C decreasing to a value of 790 MPa at 800°C. The starting temperature of the powder particle was assumed to be 200°C. Ball charged temperatures of between 100 and 250°C have been measured depending upon the apparatus and processing conditions employed. The results of this calculation are shown in figure 10. The decrease in the rate of temperature rise with true strain is due to the slight decrease in strength of the material with temperature. This curve indicates that a

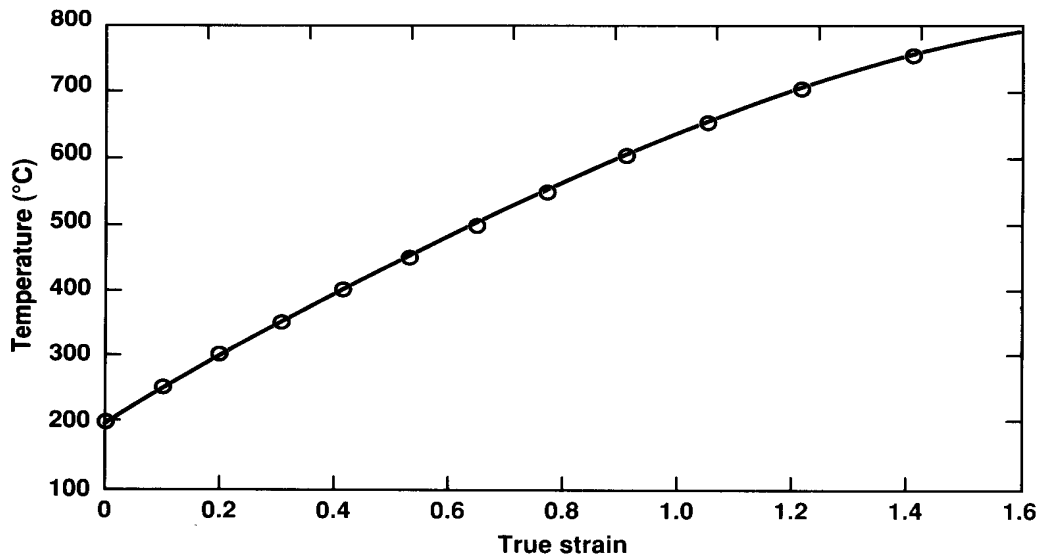


Figure 10 Calculated adiabatic temperature rise in a mechanically alloyed nickel-based superalloy during the collision event.

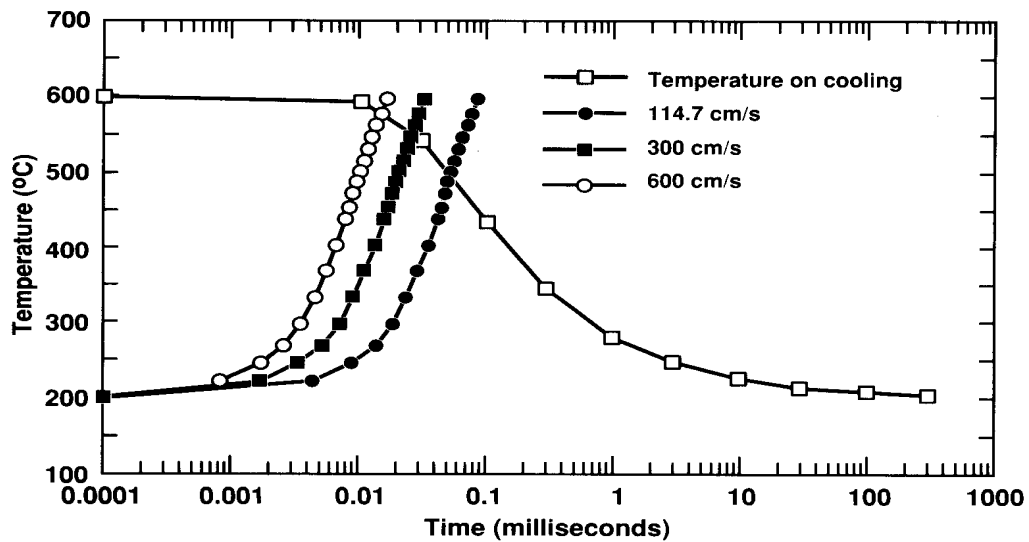


Figure 11 Cooling of the center of an 80 μm layer of metal as a function of log time. Heating rate of a 200 μm thick layer deformed at three rates is also shown.

temperature of nearly 800°C (a 600°C temperature rise) would occur for a true strain of 1.6. True strains of 0.9 to 1.25 in a single collision have been intimated from simple experiments [9]. A true strain of 0.9 would result in an adiabatic temperature of 600°C, a rise of 400°C.

The time of the collision was calculated for three cases. First, as above, by assuming that two such particles were impacted symmetrically by two grinding balls with just sufficient energy to raise the temperature to 600°C from an initial temperature of 200°C. The grinding ball 0.38 cm in diameter with a mass of 2.05 g travelling at an initial velocity of 114.7 cm/sec with a kinetic energy of 1.348×10^4 ergs would just have sufficient energy to raise the temperature of the mass of a 100 μm dia x 100 μm length of superalloy to 600°C. For each increment of strain (change in height of the particle) the time was calculated for the ball to traverse that distance at its current velocity. Increments of strain of 5 μm for the first 8 increments and 2 μm for the last 10 increments were used. The second case was for an initial velocity of the balls of 300 cm/sec as might be the case in a medium sized attrition mill. The mass of particles was increased so that the energy in the grinding balls was just sufficient to give a true strain of 0.9. The particles were assumed to form a close packed double layer between the two balls. The third example assumed an initial ball velocity of 600 cm/sec such as might be the case for collisions in a large ball mill. The estimated times for deceleration of the balls were 8.3 x

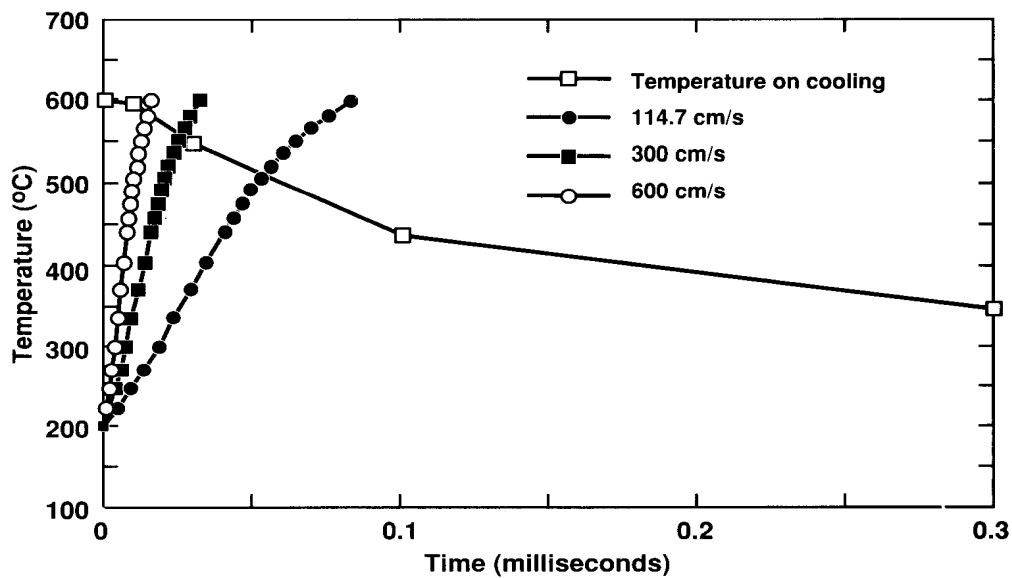


Figure 12 Cooling of the center of an 80 μm layer of metal compared to heating rate of a 200 μm thick layer during deformation at three rates.

10^{-5} sec, 3.2×10^{-5} sec and 1.6×10^{-5} sec respectively. These values range from about 10 times the value given in reference 7 to about the same value for the highest energy collision.

Next, it is instructive to check if the assumption of adiabatic conditions during the collision is correct. In order to do this, heat flow calculations were performed for the case of the slab of metal at 600°C and 40μ in semi-thickness in contact with an infinite heat sink (the grinding ball) at a temperature of 200°C . This covers the case of two 100μ thick particles or layers of particles colliding along a line of centers to a strain of 0.9. The logarithmic cooling curve for this case is shown in figure 11. Also plotted for comparison are the adiabatic heating curves as a function of time. The linear plot of this same information is shown in figure 12. Several points need to be made. First, this cooling model would break down in most cases at the end of the collision since the grinding balls would rebound from the particles due to release of the elastically stored energy in the balls and powder. Second, the rate of cooling is approximately the same as the rate of adiabatic heating for the low energy collision. A significant amount of heat would be extracted from the powder by the grinding balls as the collision occurs. Furthermore, the cooling curve is for the center of the material being deformed. Material closer to the surface of the grinding balls would cool more rapidly. In the case of the lower energy collision it is unlikely that significant portions of the material see a temperature higher than 400°C from a starting temperature of 200°C and that the maximum is probably reached in less than a tenth of a millisecond.

The cases of the higher energy collisions approach the adiabatic case. In these cases temperatures of over 500°C are probably reached and most cooling is probably much slower, by convection in the milling atmosphere as pointed out by Maurice and Courtney (8). Cases where the processed material adheres to the grinding charge, which is the case especially during the first half of processing, would more closely approach the cooling curve shown in figure 12 than the case of convective cooling.

It is interesting to consider these calculations in the light of the results of Schulz et al. [10] in which the effective temperature causing diffusion during the mechanical alloying of nickel and zirconium is estimated at 180°C . It can also be calculated for the case of nickel-chromium that homogenization of an 80% nickel-20% chromium alloy produced from elemental powders can be accounted for by interdiffusion at a temperature of 200°C , interdiffusion distances of around 0.1μ and a time of around 20 hrs, assuming that the diffusion process has an activation energy similar to that for surface diffusion in nickel. This is not unreasonable in view of the elevated dislocation and vacancy concentrations shown by others in mechanically alloyed powders.

VARIATIONS ON THE MECHANICAL ALLOYING PROCESS

In some early experiments, use was made of the adsorbed oxygen present on raw material powder surfaces and traces of oxygen added to the milling atmosphere to produce oxide dispersion strengthened superalloys by internal oxidation. Reactive metals such as lanthanum were added by including them in the nickel-aluminum-titanium master alloys. Reaction of this dispersed metal with the mechanically alloyed oxygen occurred to form lanthanum oxide dispersoids. This concept was also applied to the processing of aluminum [11,12,13]. In this variation for aluminum, now called reaction milling, organic compounds such as methanol and stearic acid or elemental carbon are used to control the extreme welding tendency of aluminum and also to add carbon and oxygen to form additional dispersoids.

It was recognized early [11] that cryogenic temperatures could be used to control the mechanical alloying process. This concept has been expanded through the use of liquid nitrogen added directly to the milling vessel [14,15] and applied to systems ranging from aluminum to nickel based superalloys. In the case of aluminum, extremely fine Al(ON) particles are reported to be formed in addition to the aluminum oxide present on the surface of the starting powders.

Mechanical alloying has been applied to prealloyed aluminum [16] for the purpose of dispersing the surface oxide within the powder particles. In a sense there were still two components in the process, although one of them was tenaciously affixed to the other rather than being a second free component. Mechanical grinding of completely prealloyed powders with no intent of introducing a second ingredient has been used by Schwarz et al. [17] to produce amorphous nickel-titanium and nickel-niobium alloys. In this case, the function of the mechanical grinding is to introduce point and lattice defects such as vacancies, interstitials, dislocations, antiphase domain boundaries, etc. to completely destroy the crystal structure and generate an amorphous material.

Shingu et al. [18] have investigated the repeated rolling of mixtures of ductile binary systems to reproduce the effects of extended ball milling. In this work, the powders were contained in stainless steel tubes which were welded and flattened prior to rolling. In each stage of the process, the thickness of the core of the flattened tube was reduced approximately twenty-fold. Optical metallography and transmission electron microscopy were used to determine the lamellar spacing as a function of the number of such cycles (see figure 13). Presumably, the rolled material was removed from the stainless steel sheath, pulverized, and recanned between cycles. Also indicated on figure 13 is the theoretical rate of refinement of structure that should have occurred. Amorphous and nanocrystalline materials were successfully produced by this process in spite of the apparent deviation of the actual lamellar thickness from theory with increasing numbers of cycles. Shingu speculated that this devia-

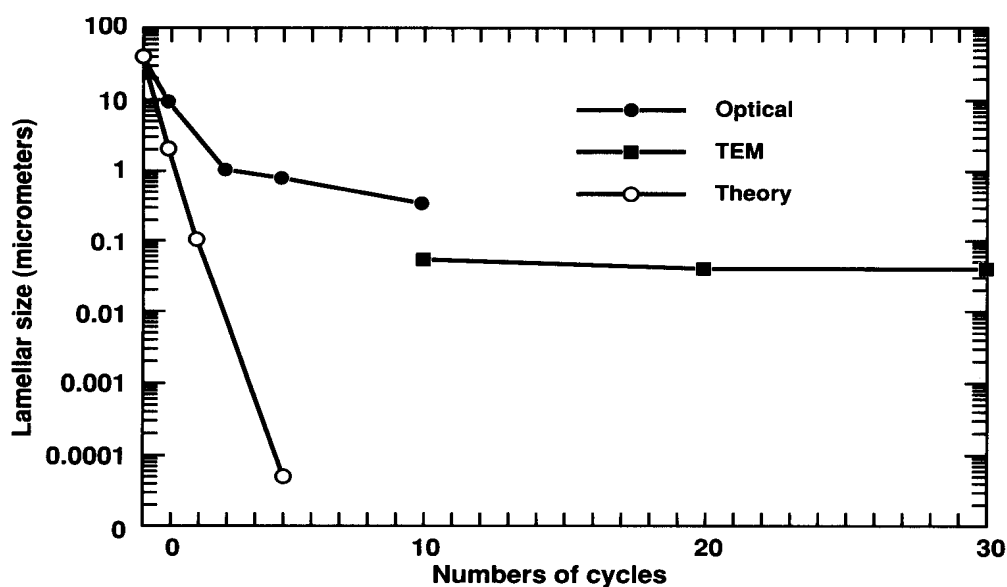


Figure 13 Refinement of structure in mechanical alloying by repeated rolling (after Shingu et al.).

tion was due to slippage of the particles within the steel sheath allowing a change in its outside dimensions without concomitant reduction in the dimensions of the particles contained therein.

The concept of chemical reactions occurring during the mechanical alloying process has been carried to an extreme by mechanically alloying large amounts of copper oxide with more reactive metals such as aluminum, titanium and iron. In this case, it was found that a thermite reaction was triggered during the mechanical alloying process [19].

SUMMARY

Recent studies on the mechanical alloying process, especially those aimed at the production of amorphous and nanocrystalline materials, have shed more light on the details of the mechanical alloying event. The mechanical alloying process, originally conceived of as a way of combining mixtures of elemental master alloy and oxide powders, has branched out into reaction milling, cryo-milling, amorphization by grinding, the use of repeated rolling and as a method of generating thermite reactions. More elaborate models for the process are being developed. This, coupled with the increased availability of numerically intense computers, suggests exciting new possibilities for the understanding of the process and its further expansion.

REFERENCES

1. J. S. Benjamin: *Sci Am.* (1976), vol. 40, p. 234.
2. B. T. McDermott and C. C. Koch: *Scripta Met.* (1986), vol. 20, p. 669.
3. E. Gaffet et al.: (1989) *New Materials by Mechanical Alloying Techniques*, p. 95, Oberursel, DGM.
4. C. C. Koch et al.: *Appl. Phys. Lett.* (1983), vol. 43, p. 1017.
5. S. K. Kang and R. C. Benn: *Met. Trans. A* (1987), vol. 18A, p. 747.
6. W. Schlump and H. Grewe: (1989) *New Materials by Mechanical Alloying*, p. 307, Oberursel, DGM.
7. T. H. Courtney et al.: (1989) *Diffusion Analysis and Applications*, p. 225, Minerals, Metals and Materials Society.
8. D. R. Maurice and T. H. Courtney: *Met. Trans. A* (1990), vol. 21A, p. 289
9. J. S. Benjamin and T. E. Volin: *Met. Trans.* (1974), vol. 5, p. 1929.
10. R. Schulz et al.: *Phys. Rev. Lett.*, (1989), 62, p. 2849.
11. J. S. Benjamin and M. J. Bomford, "Mechanically Alloyed Aluminum-Aluminum Oxide," U.S. Patent 3,816,080 (1974).
12. J. S. Benjamin and M. J. Bomford, *Met. Trans. A* (1977), vol. 8A, p. 1301.
13. G. Jangg et al.: *Aluminum* (1975), 51, p. 641.
14. R. Petkovic-Luton and J. Valone, "Method for Producing Dispersion Strengthened Metal Powders," U.S. Patent 4,647,304 (1987).
15. M. J. Luton et al.: *Mat. Res. Soc. Symp. Proc.* (1989), vol. 132, p. 79.

-
16. S. Ezz et al.: (1986), High Strength Powder Metallurgy Alloys II, p. 287, Warrendale, TMS.
 17. R. B. Schwarz and C. C. Koch, Appl. Phys. Lett. (1986), 49, p. 146.
 18. P. H. Shingu et al.: (1990), Solid State Powder Processing, p. 21, Warrendale, TMS.
 19. G. B. Schaffer and P. G. McCormick, J. of Mat. Sci. Lett. (1990), vol. 9, p. 1014.

